

Optimizing the Plasma Spray Process Parameters of Yttria Stabilized Coatings on Aluminum Alloy Using Response Surface Methodology

B.Kumaragurubaran, T.Parthipa Saravana Kumar, T.Senthil Kumar, M. Chandrasekar

Abstract- Atmospheric plasma spraying is used extensively to make Thermal Barrier Coatings of 7-8% yttria-stabilized zirconia powders. The main problem faced in the manufacture of yttria-stabilized zirconia coatings by the atmospheric plasma spraying process is the selection of the optimum combination of input variables for achieving the required qualities of coating. This problem can be solved by the development of empirical relationships between the process parameters (current, powder feed rate, stand-off distance, no of passes) and the coating quality characteristics (coating thickness, coating hardness and porosity) through effective and strategic planning and the execution of experiments by response surface methodology. This article highlights the use of response surface methodology by designing four factor five level central composite rotatable design matrixe with full replication for planning, conduction, execution, and development of empirical relationships. Further, response surface methodology was used for the selection of optimum process parameters to achieve desired quality of yttria-stabilized zirconia coating deposits on aluminum alloy.

Keywords: Plasma spray, statistical experiments, response surface methodology, yttria stabilized zirconia, coating thickness, porosity, coating hardness.

I. INTRODUCTION

Plasma-sprayed yttria-stabilized zirconia (YSZ) coatings are being increasingly used as thermal barrier coatings (TBCs) for gas turbines and diesel engines (Ref 1). Effective TBCs should exhibit low thermal diffusivity, strong adherence to the substrate, phase stability, and properties have generally been studied by means of classical one-factor-at-a-time or empirical approaches. Plasma spraying, however, involves many parameters and complex interactions among them. The one-factor-at-a-time approach requires prohibitively large numbers of trials to systematically identify the effects of the process parameters, and therefore the effects of the process parameters on the microstructure and properties of the YSZ coatings have not been fully understood yet. Statistical designs of experiments have been shown to provide efficient approaches to systematically investigate the process parameters of thermal spray. The Taguchi method was efficiently used by Kingswell et al.

Manuscript published on 30 June 2013.

* Correspondence Author (s)

B.Kumaragurubaran, Department of Mechanical Engineering, Bharathidasan Institute of Technology, Anna University, Tiruchirappalli – 620024.Tamil Nadu, India.

T.Parthipa Saravana Kumar, Department of Mechanical Engineering, Bharathidasan Institute of Technology, Anna University, Tiruchirappalli – 620024.Tamil Nadu, India.

T.Senthil Kumar, Department of Mechanical Engineering, Bharathidasan Institute of Technology, Anna University, Tiruchirappalli – 620024.Tamil Nadu, India.

M. Chandrasekar, Department of Mechanical Engineering, Bharathidasan Institute of Technology, Anna University, Tiruchirappalli – 620024.Tamil Nadu, India.

© The Authors. Published by Blue Eyes Intelligence Engineering and Sciences Publication (BEIESP). This is an open access article under the CC-BY-NC-ND license <http://creativecommons.org/licenses/by-nc-nd/4.0/>

(Ref 7) to investigate the vacuum plasma spray deposition of alumina, nickel-based alloys, and tungsten carbide/cobalt cermet coatings. The small central composite design method was employed by Wang and Coyle (Ref 8) to optimize solution precursor plasma spray process parameters to deposit NiYSZ coatings on SOFCs. Statistical design of experiment by the response surface methodology (RSM) was used to successfully optimize the micro hardness of plasma-sprayed WC-12%Co (Ref 9).

However, optimization of plasma spray process involving multiple factors and multiple responses has hardly been reported in the literature. Hence, this article deals with the application of RSM in developing empirical relationships relating important input variables, namely, the current (C), the stand-off distance (S), the powder feed rate (R), and no of passes (P), to the coating thickness ,coating hardness and the porosity of APS-YSZ TBCs (Ref 11). Further, this article illustrates how a number of over-lapping response surfaces can be used to select the operating conditions necessary to achieve the desired specifications and for the optimization of the plasma spraying process. It should be emphasized that the range selected for parameters. However, the illustrated approach and the methodology of the response surfaces are universal.

II. SCHEME OF INVESTIGATION

In order to achieve the desired objective, the present investigation was planned in the following sequence:

1. To identify the important APS process parameters;
2. To find the upper and lower limits of the identified parameters;
3. To choose the relevant experimental design matrix;
4. To conduct the experiments as per the design matrix;
5. To record the responses (measuring the tensile bond strength, lap shear bond strength, hardness, porosity, and deposition efficiency);
6. To formulate empirical relationships to predict the aforementioned responses using RSM;
7. To perform numerical and graphical optimization;
8. To conduct confirmatory test using optimized process parameters;
9. To conclude with results and discussions.

2.1 Identifying the Important Process Parameters

From the literature (Ref 19-21) and the previous study done in our laboratory, the predominant factors (APS process parameters) that have a greater influence on the coating properties were identified. They are (i) current (amps), (ii) the stand-off distance (mm), (iii) the powder feed rate (gpm), and (iv) no of passes .

2.2 Finding the Working Limits of the Parameters

A large number of spray trial runs were carried out on grit blasted 3-mm-thick AISI 316 austenitic stainless steel plates to determine the feasible working limits of APS parameters. Plasma spray deposition was carried out using an APS system 40 kW IGBT-based Plasmatron (Make: Ion Arc Technologies; India. Model: APSS-II). The feed stock was H.C. Stark, AMPERIT 827.054 powder (ZrO₂, 7% Y₂O₃) with particle size of 45 + 10 μm. The YSZ powder was directly sprayed on to the grit blasted substrate and bond coat was not used. Different combinations of APS process parameters were used to carry out the trial runs. Coating thickness for all the deposits was maintained at 300 ± 15 μm. To fix the limits of the considered factors, a couple of criteria were adopted. The criteria were that the coatings must have minimum tensile bond strength of 3 MPa and they must be deposited with a minimum deposition efficiency of 30%. During the trials, the following observations were made. (i) If the spray was carried out below 22 kW power level, then poor adhesion and subsequent delaminating of the coating were observed. If the power level was increased beyond 30 kW, then the surface evaporation from particles leading to vapor entrapment in the deposit and poor deposition efficiency were observed. (ii) If the primary gas flow rate was below 25 lpm, then anode erosion was observed, and if it was above 45 lpm, then arc blow out was observed. (iii) If the stand-off distance was less than 90 mm, then distortion of the substrate and peeling off of the coating were observed, and if it was increased beyond 130 mm, then resolidification of the molten particles resulting in poor coating adhesion and poor deposition efficiency was observed. (iv) The minimum possible powder feed rate was 15 gpm (limitation of the powder feeding system). If the powder feed rate was increased beyond 35 gpm, then a large fraction of the powder particles remain in the nonmolten condition, consequently, resulting in low spray deposition efficiency and coating delamination. (v) If the carrier gas flow rate was below 3 lpm, then the powder could not penetrate the plasma, and if it was increased beyond 11 lpm, then the powder passed right across the plasma column resulting in the erosion of anode (nozzle) edges. Nitrogen was used as secondary gas, and its flow rate was kept constant at 4 lpm.

2.3 Choosing the Experimental Design Matrix

After considering all of the aforementioned conditions, the feasible limits of the parameters were chosen so that reasonably good adherent coatings could be obtained. The yttria stabilized Zirconia (ysz) powder of coating raw materials used in this investigation was aluminum alloy. Machine experiment setup was shown in the figure 1 which was used to find the coating thickness, coating hardness, porosity level. From the literature and predominant factors which are having greater influence on coating thickness, coating hardness, porosity level coating withstanding capability were identified. They are (i) current, (ii) powder feed rate, (iii) standoff distance and (iv) Number of passes. The experiments were conducted to determine working range of above factors. The feasible limits of the parameters were chosen in such a way that the coating performance should be free from any visual effect. The important factor that are influencing the coating thickness, coating hardness,

porosity level of coating performance and their working range for yttria stabilized zirconia are presented in table 3.1. As the range of individual factor was wide, a central composite rotatable four factor, five level design matrix was selected. The experimental design matrix (table 3.2) consisting 30 sets of coded conditions and comprising a full replication of four factor factorial design of 16 points, 8 star points and 6 centre points was used. The upper and lower limits of the parameter were coded as +2 and -2 respectively. The code values for intermediate levels can be calculated from the relationship.

$$X_i = 2[2X - (X_{max} + X_{min})] / (X_{max} - X_{min})$$

Where X_i is the required coded value of variable X and X_i is any value of the variable from X_{min} to X_{max}. The performance were made as per the condition dictated by the design matrix at random order so as to avoid the noise creeping output response. As the prescribed by the design matrix 30 parameter condition were designed.

**TABLE 3.1
FEASIBLE WORKING LIMITS OF ENGINE
PROCESS PARAMETER.**

S.No	Parameters	Notation	Unit	Levels				
				(-2)	(-1)	(0)	(1)	(2)
1	Current	C	A	40	42	44	46	48
2	Powder feed rate	R	g/m	15	20	25	30	35
3	Stand off distance	S	mm	10	11	12	13	14
4	No of passes	P		1	2	3	4	5

**TABLE 3.2
DESIGN MATRIX AND EXPERIMENTAL RESULTS.**

Experiment Number	Factors				Coating thickness	Coating hardness	Porosity level
	C	R	S	p	μm	HRc	%
1	-1	-1	-1	-1	119	70	4.7
2	+1	-1	-1	-1	116	67	4.4
3	-1	+1	-1	-1	118	69	4.6
4	+1	+1	-1	-1	116	67	4.4
5	-1	-1	+1	-1	120	71	4.9
6	+1	-1	+1	-1	125	76	4.1



7	-1	+1	+1	-1	117	64	4.6
8	+1	+1	+1	-1	122	69	2.7
9	-1	-1	-1	+1	103	50	3
10	+1	-1	-1	+1	106	53	3.6
11	-1	+1	-1	+1	112	59	3.9
12	+1	+1	-1	+1	115	62	3
13	-1	-1	+1	+1	106	53	4.1
14	+1	-1	+1	+1	117	64	3.7
15	-1	+1	+1	+1	113	60	4.8
16	+1	+1	+1	+1	122	71	3.5
17	-2	0	0	0	109	58	4.3
18	+2	0	0	0	117	66	3.6
19	0	-2	0	0	110	59	4.3
20	0	+2	0	0	117	66	3.6
21	0	0	-2	0	106	55	4.3
22	0	0	+2	0	116	65	3.2
23	0	0	0	-2	126	75	4.2
24	0	0	0	+2	110	59	2.6
25	0	0	0	0	124	71	3.8
26	0	0	0	0	121	68	3.5
27	0	0	0	0	122	69	3.6
28	0	0	0	0	122	79	3.6
29	0	0	0	0	123	68	3.6
30	0	0	0	0	122	67	3.6

surface roughness Ra~ 4.0 was obtained. Three controllable parameters namely current stand – off distance and powder feed rate were indentified and plasma spraying was carried out by varying the parameters as prescribed by the design matrix and Aluminum 90% Al +10% Al₂O₃ coating was produced over Aluminum A356 substrates. The coated specimens are shown in the Figure 4.4

2.4.2. Coating Thickness Measurement

Coating thickness examinations for all the specimens were carried out by using Varsament – 3 light optical microscopes attached with climax image analyzing system (shown in Figure. 4.5) under 100X magnification. Samples were cut the required size in cross sectional direction. The cross section of the coating comprising of the base metal, the coating and interface region was polished using different grades of emery papers. Samples were etched using Keller’s reagent to reveal base metal microstructure, the interface and coating material structure remained unaltered even after etching. The microstructure of a prepared sample is shown in figure4.6



Figure 4.4 90% Al + 10% Al₂O₃ coating produced over A356 substrates



Figure 4.5 Versamet optical microscope with clemex image analyzing system

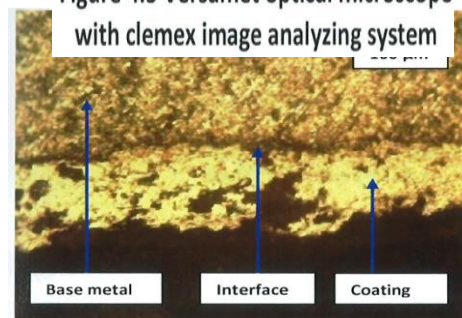


Figure 4.6 Cross – sectional view used to measure coating thickness

2.4 Conducting the Experiments

The plasma sprayed Al+10% Al₂O₃ coating was performed on Aluminum alloy plate as per the conditions dictated by the design matrix (Table 3.2). Coating thickness, coating hardness and porosity level were measured and they are presented in Table 3.2

2.4.1. Coating Preparation

The substrate (base metal – Aluminum A356) was grit blasted using 100 micron size quartz particles until a



Figure 4.7 Rockwell hardness testing machine

2.4.3. Coating Hardness Measurement

Hardness test was conducted as per the ASTM D-785 guidelines using Nobel Rockwell hardness testing machine, displayed in figure 4.7. Twenty coated specimens in addition to base material were used to investigate the hardness. The specimens were cleaned by using acetone before testing and were dried using hot air blower. Diamond indenter with load of 150kg was used to indent the specimens. The displayed result on the “c” scale of the Rockwell hardness testing machine was recorded and was noted down as hardness value for the corresponding specimen.

2.4.4. Coating Porosity Measurement

Porosity levels were measured by producing free standing coatings (specimen size 10 x 10 x 1 mm) for each set of parameters as prescribed by the design matrix. The volume percentage of porosity in case of each parameter setting were then determined using Archimedes principle.

III. PREDICTIVE MODEL FOR RESPONSE

In this study, a response surface model-building technique was utilized to predict coating thickness, coating hardness and porosity in terms of various process parameters for APS process. Details of the model-building technique are discussed below

3.1 Response Surface Methodology (RSM)

The coating thickness, coating hardness, porosity level are represented by CT, CR and PL respectively. These responses are function of current, powder feed rate, standoff distance and Number of passes and they can be expressed as

$$CT = f(C, R, S, P)$$

$$CR = f(C, R, S, P)$$

$$PL = f(C, R, S, P)$$

The second order polynomial (regression) equation used to represent the surface Y is given by

$$Y = b_0 + \sum b_i X_i + \sum b_{ii} X_i^2 + \sum b_{ij} X_i X_j + e_r \quad (1)$$

The selected polynomial for coating thickness could be expressed as

$$CT = b_0 + b_1(C) + b_2(R) + b_3(S) + b_4(P) + b_{11}(C^2) + b_{22}(R^2) + b_{33}(S^2) + b_{44}(P^2) + b_{12}(C*R) + b_{13}(C*S) + b_{14}(C*P) + b_{23}(R*S) + b_{24}(R*P) + b_{34}(S*P) \quad (2)$$

Similarly, the selected polynomial for the coating hardness of is given below

$$CR = b_0 + b_1(C) + b_2(R) + b_3(S) + b_4(P) + b_{11}(C^2) + b_{22}(R^2) + b_{33}(S^2) + b_{44}(P^2) + b_{12}(C*R) + b_{13}(C*S) + b_{14}(C*P) + b_{23}(R*S) + b_{24}(R*P) + b_{34}(S*P) \quad (3)$$

Similarly, the selected polynomial for the brake thermal efficiency of engine performance is given below

$$PL = b_0 + b_1(C) + b_2(R) + b_3(S) + b_4(P) + b_{11}(C^2) + b_{22}(R^2) + b_{33}(S^2) + b_{44}(P^2) + b_{12}(C*R) + b_{13}(C*S) + b_{14}(C*P) + b_{23}(R*S) + b_{24}(R*P) + b_{34}(S*P) \quad (4)$$

TABLE 5.1

ANOVA test result for coating thickness (df is degree of freedom ; F is fisher ratio ; p is probability).

Source	Squares	df	Mean Square	F Value	P value Prob> F	
Model	1122.283	14	80.1630952	57.487479	< 0.0001	significant
A-c	92.04167	1	92.0416667	66.005976	< 0.0001	
B-R	57.04167	1	57.0416667	40.906375	< 0.0001	
C-S	135.375	1	135.375	97.081673	< 0.0001	
D-P	345.0417	1	345.041667	247.44024	< 0.0001	
AB	0.0625	1	0.0625	0.0448207	0.8352	
AC	52.5625	1	52.5625	37.694223	< 0.0001	
AD	27.5625	1	27.5625	19.765936	0.0005	
BC	7.5625	1	7.5625	5.4233068	0.0343	
BD	85.5625	1	85.5625	61.359562	< 0.0001	
CD	3.0625	1	3.0625	2.1962151	0.1591	
A^2	117.8601	1	117.860119	84.521201	< 0.0001	
B^2	104.0744	1	104.074405	74.635031	< 0.0001	
C^2	181.5744	1	181.574405	130.21272	< 0.0001	
D^2	18.5744	1	18.5744048	13.32029	0.0024	
Residual	20.91667	15	1.39444444			
Lack of Fit	15.58333	10	1.55833333	1.4609375	0.3541	not significant
Pure Error	5.333333	5	1.06666667			
Cor Total	1143.2	29				

Std. Dev = 1.18 ; R-Squared= 0.9817 ; Mean = 116.40 ; Adj R-Squared = 0.9646 ;

C.V. % = 1.01; Pred R-Squared = 0.9148 ; PRESSn = 97.44 ; Adeq Precision = 29.192.

TABLE 5.2

ANOVA test result for coating hardness (df is degree of freedom; F is fisher ratio; p is probability)

Source	Sum of Squares	Df	Mean Square	F Value	P value Prob> F	
Model	1313.583	14	93.82738	11.49689	< 0.0001	significant
A-c	100.0417	1	100.0417	12.25834	0.0032	
B-R	40.04167	1	40.04167	4.906399	0.0427	
C-S	108.375	1	108.375	13.27944	0.0024	



D-P	532.0417	1	532.0417	65.19231	< 0.0001	
AB	0.0625	1	0.0625	0.007658	0.9314	
AC	60.0625	1	60.0625	7.359598	0.0160	
AD	33.0625	1	33.0625	4.051225	0.0624	
BC	18.0625	1	18.0625	2.21324	0.1575	
BD	138.0625	1	138.0625	16.91712	0.0009	
CD	18.0625	1	18.0625	2.21324	0.1575	
A^2	97.50298	1	97.50298	11.94727	0.0035	
B^2	85.00298	1	85.00298	10.41561	0.0056	
C^2	156.0744	1	156.0744	19.12416	0.0005	
D^2	11.0744	1	11.0744	1.356973	0.2623	
Residual	122.4167	15	8.161111			
Lack of Fit	23.08333	10	2.308333	0.116191	0.9978	not significant
Pure Error	99.33333	5	19.86667			
Cor Total	1436	29				

Std. Dev = 2.86 ; R-Squared = 0.9148 ; Mean = 65.00 ; Adj R-Squared = 0.8352;
C.V. % = 4.40; Pred R-Squared = 0.8078; PRESS = 276.00;
Adeq Precision = 13.964;

TABLE 5.3

ANOVA test result for porosity level (df is degree of freedom; F is fisher ratio; p is probability)

Source	Sum Squares	df	Mean Square	F Value	P value Prob> F	
Model	7.808	14	0.557714	2.964813	0.0225	significant
A-c	1.815	1	1.815	9.648553	0.0072	
B-R	0.426667	1	0.426667	2.268163	0.1528	
C-S	0.24	1	0.24	1.275842	0.2764	
D-P	1.215	1	1.215	6.458949	0.0226	
AB	0.7225	1	0.7225	3.840815	0.0689	
AC	0.81	1	0.81	4.305966	0.0556	
AD	0.09	1	0.09	0.478441	0.4997	
BC	0.1225	1	0.1225	0.651211	0.4323	
BD	0.4225	1	0.4225	2.246013	0.1547	
CD	1.21	1	1.21	6.432369	0.0228	
A^2	0.534405	1	0.534405	2.8409	0.1126	
B^2	0.220119	1	0.220119	1.170154	0.2965	
C^2	0.000119	1	0.000119	0.000633	0.9803	
D^2	0.114405	1	0.114405	0.608177	0.4476	
Residual	2.821667	15	0.188111			
Lack of Fit	2.821667	10	0.282167			
Pure Error	0	5	0			
Cor Total	10.62967	29				

Std. Dev.= 0.43; R-Squared = 0.7345; Mean = 3.84; Adj R-Squared = 0.4868 ;

C.V. % = 11.30; Pred R-Squared = 0.5290; PRESS = 16.25;
Adeq Precision = 7.228

Where b_0 is the average of responses and $b_1, b_2, b_3, \dots, b_{44}$ are regression coefficients that depend on respective linear, interaction, and squared terms of factors. The value of the coefficient was calculated using Design Expert Software. After determining the significant coefficients at the (95% confidence level) The final models were developed using only these coefficients and the final empirical relationship to estimate coating thickness, coating hardness, porosity level are given below

$$CT = +122.33 + 1.96 C + 1.54 R + 2.37 S - 3.79 P - 0.062 C * R + 1.81 C * S + 1.31 C * P - 0.69 R * S + 2.31 R * P + 0.44 S * P - 2.07 * C^2 - 1.95 * R^2 - 2.57 * S^2 - 0.82 * P^2 \quad (5)$$

$$CR = +70.33 + 2.04 * C + 1.29 * R + 2.12 * S - 4.71 * P + 0.063 C * R + 1.94 C * S + 1.44 C * P - 1.06 R * S + 2.94 R * P + 1.06 S * P - 1.89 C^2 - 1.76 * R^2 - 2.37 * S^2 - 0.64 * P^2 \quad (6)$$

$$PL = +3.60 - 0.28 * C - 0.13 * R - 0.10 * S - 0.23 * P - 0.2C * R - 0.22 C * S + 0.075 C * P - 0.087 * R * S + 0.16 R * P + 0.28S * P + 0.14 * C^2 + 0.090 * R^2 + 2.083E-003 * S^2 + .065 * P^2 \quad (7)$$

3.2 Checking The Adequacy Of The Model

The adequacy of the developed model was tested using the analysis of variance (ANOVA) technique and The determination of coefficient (R^2) indicates the goodness of fit for the model. In this case, the Value of determination coefficient ($R^2=0.9871$) indicates that 98.71% of the total variability is explained by the model after considering the significant factors. The models are not over fitted as indicated by the comparison of R^2 and R^2 -adjusted values. Only less than 7% of the total variations are not explained by the model. The value of adjusted determination coefficient (adjusted $R^2=0.91$) is also high, which indicates a high significant of the model. Predicted $R^2=0.91$ is in good agreement with the adjusted R^2 and shows the model would be expected to explain 90% of the variability in new data. A 'P' value less than 0.05 indicated the significant model terms. Value of probability greater than F in tables 5.1, 5.2 and 5.3 for the model is less than 0.05, which indicates that the model is significant. Lack of fit is insignificant and therefore indicates that the model fits well with the experimental data. The high P value for the lack of fit test also indicates that the model does adequately fit with the response surface for coating thickness. All the above considerations indicate on excellent adequacy of the regression model. Each observed value is compared with the predicted value calculated from the model in figures 6.1, 6.2 and 6.3.

IV. RESULT AND DISCUSSION

The response surface methodology (RSM) was used to optimize the coating parameters in the study. RSM is a collection of mathematical and statistical techniques that are useful for designing a set of experiments, developing a mathematical model, analyzing for the optimum combination of input parameters, and expressing the values graphically.



To obtain the influencing nature and optimized condition of the process on coating thickness, coating hardness and porosity level the surface plots and contour plots which are the indications of possible independence of factors have been developed for the proposed empirical relation by considering two parameters in the middle level and two parameters in the X and Y axes as shown in figures 6.7, 6.8 and 6.9 respectively. These response contours can help in the prediction of the response for any zone of the experimental domain.

The apex of the response plots show the maximum achievable coating thickness, coating hardness and minimum porosity in figure 6.7, 6.8 and 6.9. The coating thickness and coating hardness and porosity increases with increasing the current, feed rate and increasing the stand of distance but certain level only after decrease. A contour plot is produced to display the region of the optimal factor settings visually. For second order responses, such a plot can be more complex compared to the simple series of the parallel lines that can occur with first order models. Once the stationary point is found, it is usually necessary to characterize the response surface in the immediate vicinity of the point. Characterization involves identifying whether the stationary point is a minimum response or maximum response or via saddle point. To classify this, it is most straightforward to examine it through a contour plot. Contour plots play a very important role in the study of a response surface. It is clear from figures 6.4, 6.5 and 6.6 that the coating thickness, coating hardness and porosity level increases with increasing the feed rate and fuel stand of distance to a certain value and then decreases but the coating thickness and coating hardness increases with increasing the current.

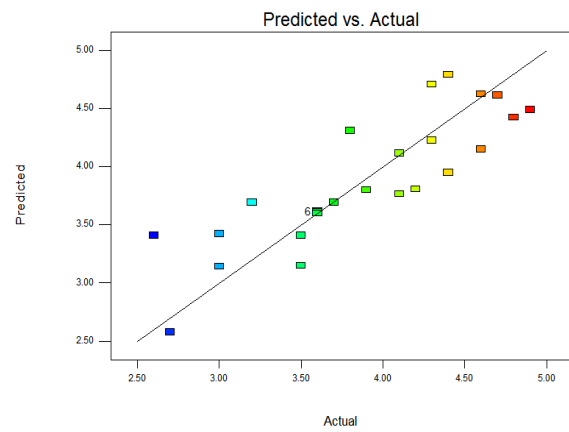


Fig.6.3 Normal probability plot of experimental versus predicted

RSM is used to find the optimal set of process parameters that produce a maximum or minimum value of the response. By analyzing the response surfaces and contour plots (figs.6.4-6.9), the maximum achievable coating thickness, coating hardness and porosity level values are found to be 122.33 μ m, 70.333HRc and 3.6 % respectively. The corresponding process parameter that yielded this maximum value current 440A, powder feed rate 25g/min, stand of distance 120mm and no of passes 4. Using these optimized coating process parameters arranged in machine equipment and then tested. The values of coating thickness, coating hardness and porosity level are found to be 124 μ m, 71HRc and 3.6%. From these values, it is inferred that the predicted and experimental optimized strength values are in good agreement and the variations is found to be $\pm 6\%$.

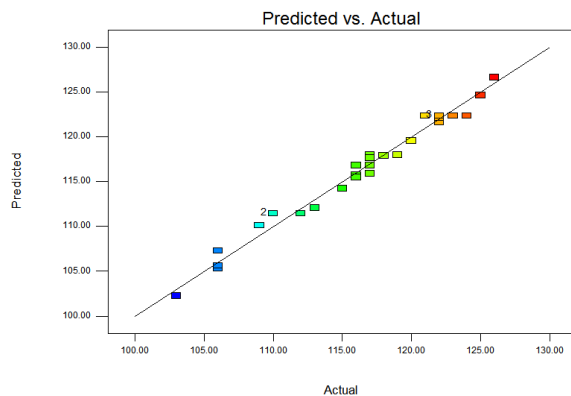


Fig.6.1. Normal probability plot of experimental versus predicted coating thickness

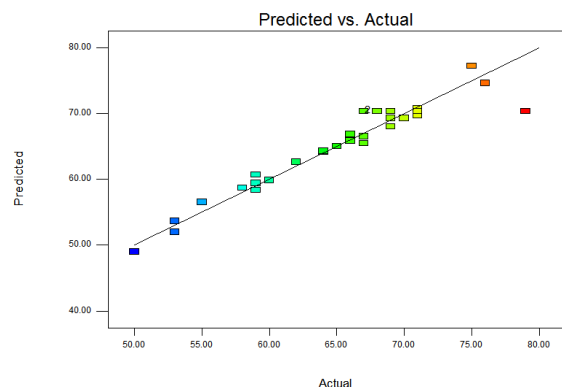


Fig 6.2 Normal probability plot of experimental versus predicted coating hardness

V. PROCESS OPTIMIZATION

To investigate the influencing tendency of the process parameters on the responses, 3D graphs were plotted under certain processing conditions. The 3D response surface and 2D contour plots are the graphical representations of the regression equations used to determine the optimum values of the variables within the ranges considered. Furthermore, a contour plot is produced to display the region of the optimal factor settings visually. For second-order response surfaces, such a plot can be more complex compared to the simple series of parallel lines that can occur with first order empirical relationships. Once the stationary point is found, it is usually necessary to characterize the response surface in the immediate vicinity of the point. Characterization involves identifying whether the stationary point found is a minimum response or maximum response or a saddle point. To classify this, it is most straightforward to examine it through a contour plot.

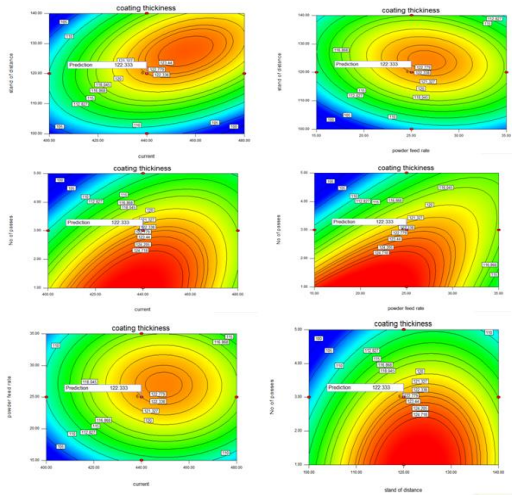


Fig 6.4 contour graphs for coating thickness

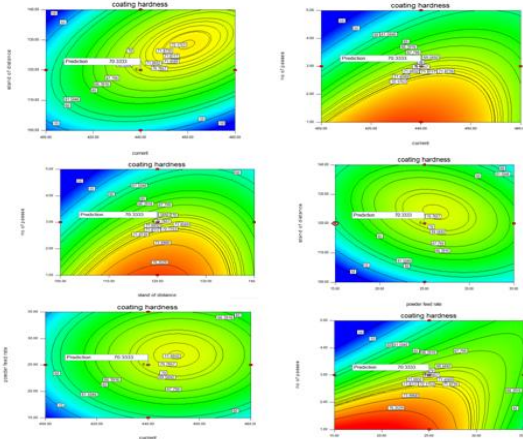


Fig 6.5 contour graphs for coating hardness

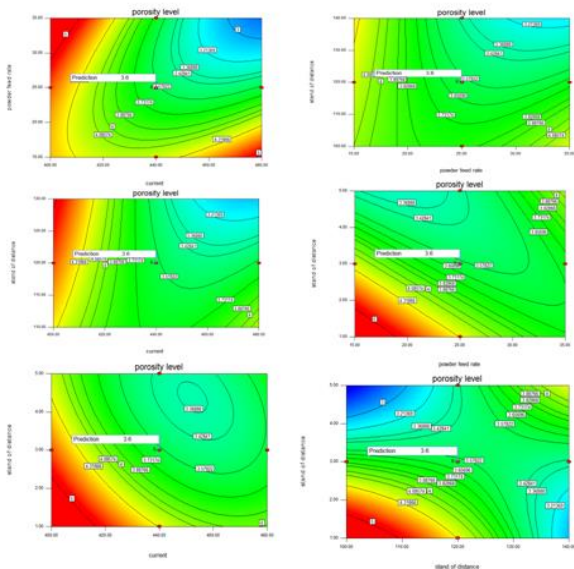


Fig 6.6 contour graphs for porosity level

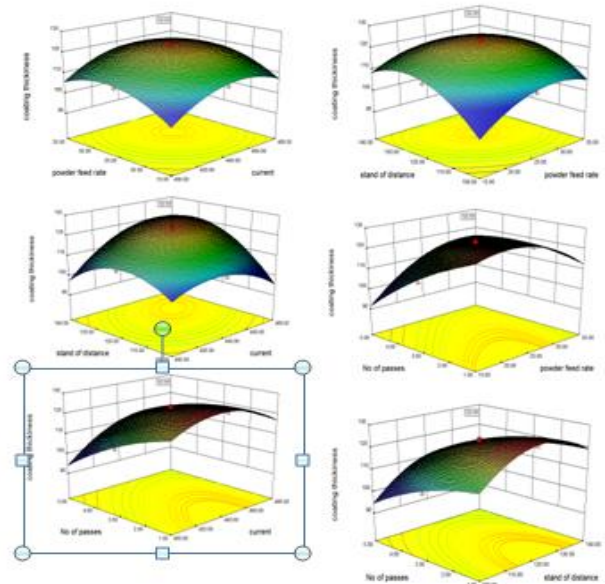


Fig 6.7 response graphs for coating thickness

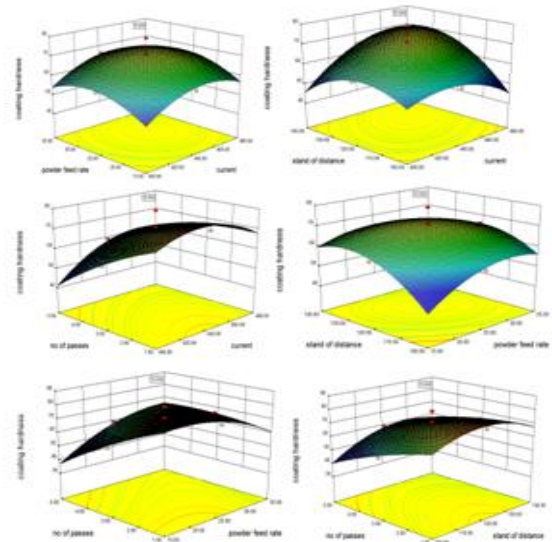


Fig 6.8 Response graphs for coating hardness

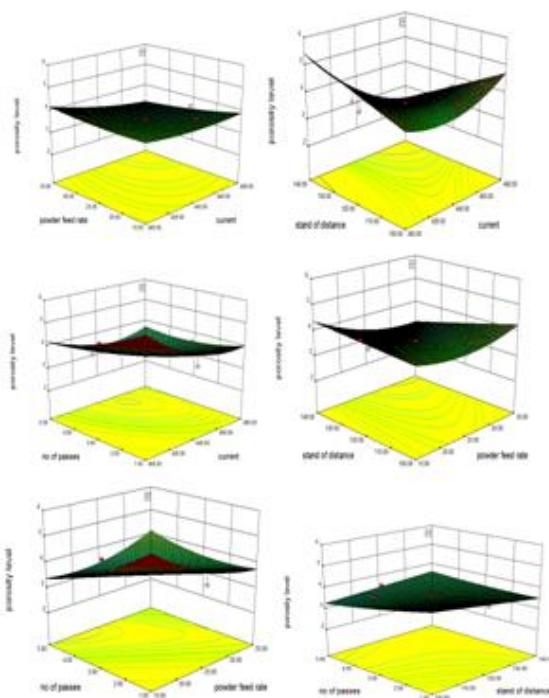


Fig 6.9 response graphs for porosity level

Contributions made by the process parameters on effect of the coating thickness, coating hardness and porosity level can be ranked from their respective 'F' ratio value which was presented in table 8 provided the degrees of freedom are same for all input parameters. The higher F ratio value implies that the respective term is more significant and vice versa. From the F ratio values, it can be concluded that current is contributing more on coating thickness, coating hardness and porosity level it is followed by powder feed rate, stand of distance, no of passes for the range considered in this investigation.

Estimated regression coefficients for coating thickness, coating hardness and porosity level

Factor	Estimated coefficients		
	coating thickness	coating hardness	porosity level
Intercept	122.3333333	70.33333333	3.6
A-c	1.958333333	2.041666667	-0.275
B-R	1.541666667	1.291666667	-
C-S	2.375	2.125	0.1333333333
D-P	-3.791666667	-4.708333333	-0.225
AB	-0.0625	0.0625	-0.2125
AC	1.8125	1.9375	-0.225
AD	1.3125	1.4375	0.075
BC	-0.6875	-1.0625	-0.0875
BD	2.3125	2.9375	0.1625
CD	0.4375	1.0625	0.275
A ²	-2.072916667	-1.885416667	0.139583333
B ²	-1.947916667	-1.760416667	0.089583333
C ²	-2.572916667	-2.385416667	0.002083333
D ²	-0.822916667	-0.635416667	0.064583333

VI. CONCLUSIONS

The following important conclusions are obtained from this investigation.

1. Empirical relationship were developed to predict the Coating thickness, Coating Hardness and Porosity of process parameter .the developed relationship can be effectively used to predict the Coating thickness, Coating Hardness and Porosity at 95 % confidence level.
2. A maximum Coating thickness of 122.33µm, Coating Hardness of 70.33HRc and Porosity of 3.6% could be attained under the process condition of 440amps current, 25g/min of powder feed rate, 120mm stand of distance and 3 of number of passes .
3. The experimentally determined Coating thickness, Coating hardness and Porosity were found to be 124µm,71HRc and 3.6% respectively which shows the consistency of model.

REFERENCES

- [1] T. Beck, R. Herzog, O. Trunova, M. Offermann, R.W. Steinbr-ech, and L. Singheiser, Damage Mechanisms and Lifetime Behavior of Plasma-Sprayed Thermal Barrier Coating Systems for Gas Turbines. Part II. Modeling, Surf. Coat. Technol., 2008, 202, p 5901-5908
- [2] J. Go´mez-Garci´a, A. Rico, M.A. Garrido-Maneiro, C.J. Mu´nez, P. Poza, and V. Utrilla, Correlation of Mechanical Properties and Electrochemical Impedance Spectroscopy Analysis of Thermal Barrier Coatings, Surf. Coat. Technol., 2009, 204, p 812-815
- [3] S.-I. Jung, J.-H. Kim, J.-H. Lee, Y.-G. Jung, U. Paik, and K.-S.Lee, Microstructure and Mechanical Properties of Zirconia-Based Thermal Barrier Coatings with Starting Powder Mor-phology, Surf. Coat. Technol., 2009, 204, p 802-806
- [4] S.A. Sadeghi-Fadaki, K. Zangeneh-Madar, and Z. Valefi, The Adhesion Strength and Indentation Toughness of Plasma-Sprayed Yttria Stabilized Zirconia Coatings, Surf. Coat. Technol., 2010, 204, p 2136-2141
- [5] P. Diez and R.W. Smith, The Influence of Powder Agglomeration Methods on Plasma Sprayed Yttria Coatings, J. Therm. Spray Technol., 1993, 2, p 165-172
- [6] A. Kulkarni, A. Vaidya, A. Goland, S. Sampath, and H. Herman, Processing Effects on Porosity-Property Correlations in Plasma Sprayed Yttria-Stabilized Zirconia Coatings, Mater. Sci. Eng. A, 2003, 359, p 100-111
- [7] R. Kingswell, K.T. Scott, and L.L. Wassell, Optimizing the Vacuum Plasma Spray Deposition of Metal, Ceramic and Cermet Coatings Using Designed Experiments, J. Therm. Spray Technol., 1993, 2, p 179-186
- [8] Y. Wang and T.W. Coyle, Optimization of Solution Precursor Plasma Spray Process by Statistical Design of Experiment, J. Therm. Spray Technol., 2008, 17, p 692-699
- [9] Troczynski and M. Plamondon, Response Surface Methodology for Optimization of Plasma Spraying, J. Therm. Spray Technol., 1992, 1, p 293-300
- [10] F.H. Yuan, Z.X. Chen, Z.W. Huang, Z.G. Wang, and S.J. Zhu, Oxidation Behavior of Thermal Barrier Coatings with HVOF and Detonation-Sprayed NiCrAlY Bondcoats, Corros. Sci., 2008, 50, p 1608-1617
- [11] E. Lugscheider, F. Ladru, V. Gourlaouen, and C. Gualco, Enhanced Atmospheric Plasma Spraying of Thick TBCs by Improved Process Control and Deposition Efficiency, Thermal Spray: Meeting the Challenges of the 21st Century, C. Coddet, Ed., May 25-29, 1998 (Nice, France), ASM International, 1998, 1693 p
- [12] J. Wigren and L. Pejryd, Thermal Barrier Coatings-Why, How, Where and Where to, Thermal Spray: Meeting the Challenges of the 21st Century, C. Coddet, Ed., May 25-29, 1998 (Nice, France), ASM International, 1998, 1693 p



- [13] K.C. Chang, W.J. Wei, and C. Chen, Oxidation Behavior of Thermal Barrier Coatings Modified by Laser Remelting, Surf. Coat. Technol., 1998, 102, p 197-204
- [14] P.-C. Tsai, J.-H. Lee, and C.-L. Chang, Improving the Erosion Resistance of Plasma-Sprayed Zirconia Thermal Barrier Coatings by Laser Glazing, Surf. Coat. Technol., 2007, 202, p 719-724
- [15] M. Prystay, P. Gougeon, and C. Moreau, Structure of Plasma-Sprayed Zirconia Coatings Tailored by Controlling the Temperature and Velocity of the Sprayed Particles, J. Therm. Spray Technol., 2001, 10, p 67-75
- [16] M. Friis, C. Persson, and J. Wigren, Influence of Particle In-Flight Characteristic on the Microstructure of Atmospheric Plasma Sprayed Yttria Stabilized ZrO₂, Surf. Coat. Technol., 2001, 141, p 115-127
- [17] A. Kucuk, R.S. Lima, and C.C. Berndt, Influence of Plasma Spray Parameters on In-Flight Characteristics of ZrO₂-8(wt.%)Y₂O₃ Ceramic Particles, J. Am. Ceram. Soc., 2001, 84, p 685-692
- [18] A. Kucuk, R.S. Lima, and C.C. Berndt, Influence of Plasma Spray Parameters on Formation and Morphology of ZrO₂-8(wt.%)Y₂O₃ Ceramic Particles, J. Am. Ceram. Soc., 2001, 84, p 693-700
- [19] R. Suryanarayanan, Plasma Spraying: Theory and Applications, World Scientific Publishing, New York, 1993
- [20] R.B. Hiemann, Plasma-Spray Coating-Principles and Applications, Wiley VCH Publishers Inc., New York, 1996
- [21] L. Pawlowski, The Science Engineering of Thermal Spray Coatings, 2nd ed., John Wiley & Sons Ltd, London, 2008